Individualized psychiatric imaging based on inter-subject neural synchronization in movie watching

Zhi Yang [a,b,c,d,*], Jinfeng Wu [e,f], Lihua Xu [a], Zhengzheng Deng [c,e,f], Yingying Tang [a], Jiaqi Gao [e,f], Yang Hu [a,c], Yiwen Zhang [a,c], Shaozheng Qin [g,**], Chunbo Li [a,b,d], Jijun Wang [a,b,d,***]

[a] Shanghai Key Laboratory of Psychotic Disorders, Shanghai Mental Health Center, Shanghai Jiao Tong University School of Medicine, Shanghai, China
[b] Institute of Psychological and Behavioral Science, Shanghai Jiao Tong University, Shanghai, China
[c] Laboratory of Psychological Heath and Imaging, Shanghai Mental Health Center, Shanghai Jiao Tong University School of Medicine, Shanghai, China
[d] Brain Science and Technology Research Center, Shanghai Jiao Tong University, Shanghai, China
[e] CAS Key Laboratory of Behavioral Science, Institute of Psychology, Beijing, China
[f] Department of Psychology, University of Chinese Academy of Sciences, Beijing, China
[g] State Key Laboratory of Cognitive Neuroscience and Learning & IDG/McGovern Institute for Brain Research, Beijing Normal University, Beijing, China

ARTICLE INFO

ABSTRACT

The individual heterogeneity is a challenge to the prosperous promises of cutting-edge neuroimaging techniques for better diagnosis and early detection of psychiatric disorders. Individuals with similar clinical manifestations may result from very different pathophysiology. Conventional approaches based on comparing group-averages provide insufficient information to support the individualized diagnosis. Here we present an individualized imaging methodology that combines naturalistic imaging and the normative model. This paradigm adopts video clips with rich cognitive, social, and emotional contents to evoke synchronized brain dynamics of healthy participants and builds a spatiotemporal response norm. By comparing individual brain responses with the response norm, we could recognize patients using machine learning techniques. We applied this methodology to recognize first-episode drug-naïve schizophrenia patients in a dataset containing 72 patients and 54 healthy controls. Some segments of the video evoked more synchronized brain activity in the healthy controls than in the schizophrenia patients. We built a spatiotemporal response norm by averaging the brain responses of the healthy controls in a training set, and trained a classifier to recognize patients based on the differences between individual brain responses and the norm. The performance of the classifier was then evaluated using an independent test set. The mean accuracies from a 5-fold cross-validation were 0.71–0.78 depending on the parameters such as the number of features and the width of the sliding windows. These findings reflected the potential of this methodology towards a clinical tool for individualized diagnosis.

1. Introduction

Brain imaging has been expected to benefit translational psychiatry by providing unique information for better diagnosis and early detection of psychiatric disorders. The main body of imaging research has tackled this challenge by comparing a group of patients with the same clinical diagnosis category to a healthy group, attempting to detect common and generalizable brain deficits for diagnosis of a particular type of mental disorder (Spaulding and Deogun, 2011). This design implicitly assumed that patients with similar clinical manifestations share common neural characteristics (Kapur et al., 2012). However, considerable individual heterogeneity in psychiatric disorders has induced difficulties in the search for accurate and reliable neuroimaging markers (Insel et al., 2010). A brain structural study has revealed that although the large sample helped to detect significant group differences between mental disorders and normal population, only 2% of the patients with the same diagnosis showed common brain structural abnormalities (Wolfers et al., 2018).

An approach to detect individualized deficits in mental disorders is

the normative model. This model characterizes the mean and variability of the mentally healthy population and compares individual brains to the healthy norm to yield individualized inferences. This model is a promising strategy for precision psychiatry because it avoids averaging brain features across patients and therefore helps to reflect individual-specific brain deficits (Braga and Buckner, 2017; Gordon et al., 2017; Wang et al., 2018). Such a strategy has recently been applied to examine individualized structure abnormalities in bipolar disorder and schizophrenia (Wolfers et al., 2018).

Compared to structural metrics, functional imaging has an advantage in the application of this normative model: proper stimuli in functional imaging may reduce the individual difference of the healthy population and reveal a larger difference between mental disorder patients and the "healthy norm". Previous studies have found larger individual differences in brain functional connectivity in associative cortices that involved in complicated information integration (Mueller et al., 2013). Thus, compared with resting-state, a paradigm with rich social and cognitive stimuli that evoke higher-level information processing is a better candidate for a normative model to reveal the abnormal brain response in individual mental disorder patients (Finn et al., 2017).

This study presents a methodology that combines naturalistic imaging with the normative model. We aim to elaborate on the difference of brain responses between individual psychiatric patients and mentally healthy participants, so that the patients could be identified from a movie-watching brain scan. Compared with brain features such as anatomical structure, resting-state functional connectivity, and brain responses to repetitive, single-cognitive domain tasks, the naturalistic paradigm is a more ecological fMRI design that engages neural circuits in natural contexts (Hasson, 2004; Nguyen et al., 2019). Previous studies have shown that movies with rich emotional and real-life context effectively evoked synchronization of brain responses from healthy population (Lahnakoski et al., 2014; Isik et al., 2018; Finn et al., 2017). Further, studies have suggested that individuals with mental disorders could exhibit different brain response patterns from healthy controls when viewing a movie (Byrge et al., 2015; Carlson et al., 2017). Therefore, we hypothesize that the naturalistic paradigm has the potential to reduce the individual variability of mentally healthy participants. Further, by comparing individual brain responses with the "healthy norm" evoked by the naturalistic paradigm, we could recognize patients using machine learning techniques. In this paper, we examine whether schizophrenia patients could be identified using this individualized approach.

2. Methods

2.1. Participants

Seventy-four first-episode drug-naive individuals with schizophrenia were recruited from the Shanghai Mental Health Center in China, and 58 healthy control participants were recruited from local communities in the same city. The Institutional Review Board at the Shanghai Mental Health Center approved the study protocol. Written informed consent was obtained from each participant or his/her guardian prior to data acquisition. The inclusion criteria for the patients were: (1) age 16 to 40; (2) a consensus diagnosis by two research psychiatrists of first-episode schizophrenia according to the DSM-IV on the basis of a Structured Clinical Interview; (3) an academic degree higher than middle school and capable of completing all study assessments; and (4) antipsychotic naive. The exclusion criteria were: (1) mania or inability to finish study assessments; (2) major depression according to DSM-IV; (3) a score of 7 or higher on the Calgary Depression Scale for Schizophrenia (CDSS); (4) a history of suicidal behavior; (5) a history of substance abuse; (6) pregnancy; (7) a history of serious physical disease; (8) a contraindication for MRI scans, for instance, with metal implants. To rule out the effect of the medication, the patients did not take medicine before the MRI scans, and they received regular pharmacological treatments after the scan. The time from enrolment was usually 2–3 days and no more than a week.

The inclusion criteria for age- and gender-matched healthy control group were: (1) age 15–40; (2) no serious physical diseases, pregnancy, or substance abuse; (3) no psychoactive substance for at least one month; (4) no history of mental disorder; and (5) academic degree higher than primary school. The exclusion criteria for healthy controls were: (1) meeting criteria for any mental disorder according to DSM-IV; (2) a family history of mental disorder; (3) unstable mental state; (4) a history of taking any antipsychotic drugs; (5) a history of substance abuse; (6) pregnancy; (7) a history of serious physical diseases; (8) a contraindication for MRI scans.

With these criteria, a total of 126 participants were recruited, including 72 individuals with schizophrenia (SZ, 24 females), and 54 normal controls (NC, 23 females). For the SZ group, the mean age was 23.4, the mean education years was 11.6, and the mean PANSS (Positive and Negative Syndrome Scale) score was 71.90; For the NC group, the mean age was 23.5, the mean education years was 14.8.

2.2. Video stimuli

A silent video clip consisting of 6 public-interest advertisements was used in this study. The length of the advertisements ranged between 30″ to 2′01″, and the total length of the video clip was 7′49″ (Supplementary Table 1). While the audio is an important element of the video clip, due to the narrow diameter of the 32-channel coil, we were not able to fit a headphone in it. Nonetheless, a silent video was free of confounders due to language differences. The video and corresponding rating scores are shared at https://github.com/yangzhi-psy/naturalistic_scz.

2.3. Data acquisition

All imaging data were collected with a 3.0 T S Verio MRI scanner (Enlargen, Germany) at the Shanghai Mental Health Center. Resting-state scans were acquired using a multi-band echo-planar imaging (MB-EPI) sequence (50 axial slices), FOV = 216 mm, matrix = 72×72, slice thickness/gap = 3.0/0.0 mm, TR/TE = 2000/30 ms, flip angle = 85, 240 vol, duration 8′00″. High-resolution anatomical scans were acquired with a T1-weighted 3D MP-RAGE sequence (192 sagittal slices, FOV = 256 mm, matrix = 256×240, slice thickness/gap = 1.0/0.0 mm, TR/TE/TI = 2300/2.96/900 ms). Before the scan, the participants were instructed to keep their head still and pay close attention to the video. After scanning, the participants were asked to report their feelings during the scan, such as falling into sleep, not watching the video, and any other uncomfortable feeling. Participants reporting sleep or not watching the video during the functional scans were excluded from this study.

2.4. Image preprocessing and quality control

The following preprocessing steps were applied to the fMRI data: (1) the first 5 vol were discarded to allow MRI signal equilibration; (2) the head movements were realigned over the entire scan; (3) nuisance artifacts such as the 24-parameter head motion time series, the mean signals of the white matter and ventricles, and head motion spikes were regressed out from voxel-wise time series; (4) the fMRI image was spatially normalized to MNI152 space using ANTs, by combining a rigid transformation from the mean fMRI image to the individual's structural image and a nonlinear transformation to a MNI152 template; (5) the 4D data were standardized to a global mean intensity of 10,000; (6) the data were then spatially smoothed using a 6-mm FWHM Gaussian kernel.

The quality of brain extraction and registration was visually checked. Participants with poor brain registration quality and large head motion were excluded from further analysis. Head motion was evaluated using mean framewise displacement (meanFD), and the maximal meanFD was limited to 0.2 mm.

2.5. Sliding-window inter-subject correlation analysis

As demonstrated in Fig. 1, we split the preprocessed fMRI data into a
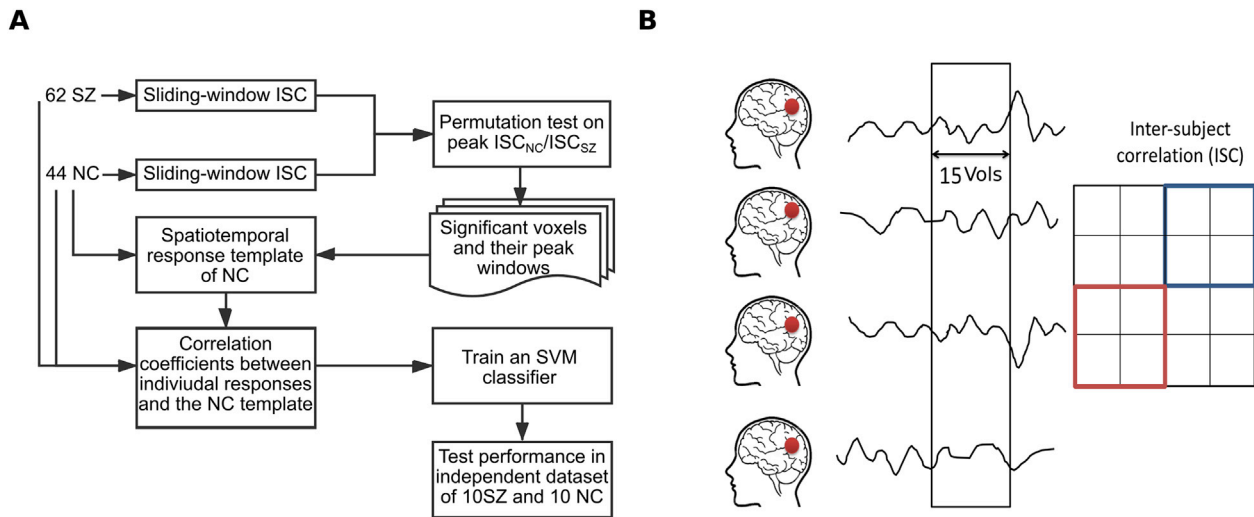
Fig. 1. Flowcharts of the analyses. (A) An overview of the analyses. The analysis consisted of a training stage (red rectangle) and a test stage (blue rectangle). The data for the two stages were independent. In the training stage, we calculated voxel-wise sliding-window inter-subject correlation analyses (ISC) in 62 schizophrenia (ISC_{SZ}) and 44 normal control (ISC_{NC}) individuals. The peak ISC_{NC}/ISC_{SZ} ratios between the two groups were as examined using a permutation test with multiple comparison correction. For the supra-threshold voxels, the BOLD signals in the time windows with the peak ISC_{NC}/ISC_{SZ} values were averaged across the NC individuals, yielding "NC templates" of brain responses. The BOLD signals of each individual, including both NC and SZ, were correlated with the 'NC templates'. Then a linear classifier based on support vector machine was trained to classify SZ and NC individuals based on the correlation coefficients. In the test stage, we evaluated the performance of the classifier using the independent test dataset containing 10 SZ and 10 NC individuals. (B) A flowchart of the sliding-window ISC analysis. The time series of the voxels at the same voxels were split into sliding windows. Within each time window, a correlation matrix was computed. ISC_{NZ} and ISC_{SZ} were computed by averaging inter-subject correlations in the NC and SZ groups, respectively.

discovery dataset (62 SZ, 20 females; 44 NC, 20 females) and a verification dataset (10 SZ, 2 females; 10 HC, 5 females). The 10 SZ and 10 NC participants in the verification were randomly selected and matched in age and education years. A flowchart of the analyses is presented in Fig. 1. For each participant in both datasets, the voxel-wise time series were segmented into overlapping time windows. The width of each window was 15 vol (30s), and the overlap between windows was 14 vol (2s). This procedure yielded 221 segments of time series for each voxel and each participant.

The following procedures were only applied to participants in the discovery dataset. Inter-subject correlation coefficients were computed using these segments, i.e., the time series in the corresponding time windows at the same locations of different participants were correlated. To simplify further analyses, we adjusted the correlation coefficients to non-negative values by adding 1, so that the similarity metric ranged between 0 and 2. We then calculated the mean inter-subject correlation for the SZ group in the discovery set (ISC_{SZ}) and the NC group in the discovery set (ISC_{NC}) by summing up all pairwise correlation coefficients among the group members. The ISC_{SZ} and ISC_{NC} characterize the extent of the brain activity synchronization among the SZ and NC participants, respectively. The difference between ISC_{SZ} and ISC_{NC} was presented by dividing ISC_{NC} by ISC_{SZ}. ISC_{SZ}, ISC_{NC}, and their ratio were functions of space and time because the correlations were performed on each sliding window and each voxel in the brain.

To search for brain regions with large ISC_{NC}/ISC_{SZ} ratios, we first represented each voxel using the maximal ISC_{NC}/ISC_{SZ} ratio across the 221 sliding windows. Next, we generated a null-distribution of the maximal ISC_{NC}/ISC_{SZ} ratios by randomly permuting the participants among the NC and SZ groups (fixed the numbers of participants for both groups, number of permutations $= 5000$). With this distribution, the significance of the maximal ISC_{NC}/ISC_{SZ} ratios obtained in the real data was evaluated. To correct for multiple comparison error, we set the threshold for the voxel-wise at $p < 0.005$ (single-tailed) and determined the spatial-extent threshold for significant clusters (88 voxels) using a Monte-Carlo simulation. The smoothness used in the simulation was estimated using the maximal ISC_{NC}/ISC_{SZ} ratio map. This procedure was also applied to examine the significance of ISC_{SZ} and ISC_{NC}

2.6. Feature extraction and classification

The above analyses identified voxels with significantly large ISC_{NC}/ISC_{SZ} ratios in the discovery dataset, suggesting that brain activity measured in these voxels were more synchronized in NC than SZ participants. We further identified the peak sliding window (showing maximal ISC_{NC}/ISC_{SZ} ratio) for each of these significant voxels. The BOLD signal within these peak sliding windows was then averaged across 44 NC participants to generate a spatiotemporal template of synchronized brain activities for NC. For each participant, the time series located in the corresponding time windows of the corresponding voxels identified above were extracted and correlated to the NC templates. The resultant correlation coefficients indicate the similarity, at the specified spatiotemporal locations, between the brain activity of the participants and the NC template. These correlation coefficients were used as features for classification.

A support vector machine (SVM) with linear kernel was trained to identify SZ patients using the correlation coefficients obtained in the discovery dataset. To examine the performance, we applied the classifier to the verification dataset that is independent of the discovery dataset. Classification accuracy, sensitivity, and specificity to identify SZ patients were calculated based on the predictions of the classifier.

We further examined the generalization of the classification model by using a 5-fold cross-validation scheme. All the data were pooled and randomly split into 5 folds, with each fold contained around 85 individuals for training and 21 for test. The group ratio was kept similar across the training set of the 5 folds. The feature selection procedures were only applied to the training set in each fold. To reduce the computational demand, we did not perform the permutation tests as described above. Instead, we ranked the voxels according to the ISC_{NC}/ISC_{SZ} ratios as defined above. For each fold, the ISC_{NC}/ISC_{SZ} ratios were re-computed only in the training set, and the voxels with the largest ISC_{NC}/ISC_{SZ} ratios were selected to build a response template of NC individuals using the same procedure described above. The correlation coefficients of every individual to this response template were used to train the SVM classifier. In the test set, all the individuals were correlated to this response template, and the classifier predicted the label of the

individuals based on the correlation coefficients. Using this scheme, we also examined the effects of the width of the sliding-window (15 vol, 30 vol, 60 vol, and the whole time series) and the proportion of the selected voxels in the ISC_{NC}/ISC_{SZ} ranking (top 1%, 3.5%, 5%, 10%, 20% and 30%).

3. Results

3.1. Naturalistic paradigm evokes higher inter-subject correlation in normal controls

To examine whether the naturalistic stimuli evoked higher inter-subject correlation in the NC group than in the SZ group, we first compared the peak of the sliding-window inter-subject correlations (maxISCs) between the two groups in voxel, region, and network levels (Fig. 2). At the voxel level, NC and SZ showed comparable ISCs in visual areas, but NC showed higher maxISCs in the temporal, parietal and dorsal frontal lobes than SZ (Fig. 2A–B). When averaging the maxISCs into 264 brain regions (Power et al., 2010), we observed a number of regions showing significantly higher maxISCs in NC than in SZ (Fig. 2C, paired t = 17.88, p < 0.001). When averaging the maxISCs into the 7 intrinsic networks proposed by Thomas Yeo et al. (2011), NC exhibited higher maxISCs than SZ in all networks (Fig. 2D). The difference between NC and SZ became smaller when calculating the inter-subject correlation using the entire time series (Fig. 2E–F). These findings suggest that the naturalistic stimuli evoked higher homogeneity in the NC than SZ groups. The sliding-window approach evoked larger between-group difference in inter-subject correlation than the static ISC approach that computes the ISC using the entire time series.

3.2. Spatiotemporal characteristics of the group difference of ISC

Using permutation tests, we identified 11 clusters, containing 2038 voxels, in which the temporal maxima of ISC_{NC}/ISC_{SZ} ratios were significantly larger than the chance level (voxel-wise p < 0.005, one-tailed, cluster size > 88 voxels, family-wise error p < 0.05), indicating that brain activities in these voxels were significantly more synchronized (at some time points) in the NC than in the SZ groups. As shown in Fig. 3A and Supplementary Table 2, these clusters located in the right precuneus, left middle temporal gyrus, left inferior parietal lobule, right inferior parietal lobule, left superior frontal gyrus, right supramarginal gyrus, right middle frontal gyrus (BA8), right middle frontal gyrus (BA6), right cerebellum (uvula), left superior temporal gyrus, and left inferior frontal gyrus, indicating that some activities in these regions are significantly more synchronized in NC subjects.

As a control condition, we examined the ISC in a voxel located in the primary visual area (at the center of the pink circle in Fig. 3A) and found no significant ISC_{NC}/ISC_{SZ}. Fig. 3B demonstrates that the ISC time courses for the NC and SZ groups are similar, ruling out the possibility that the SZ participants failed to watch the video. We also examined whether the group differences were due to the different levels of head motion of the two groups during the scan. We applied the same sliding windows to compute the mean FD within each of them. The results are presented in Supplementary Fig. S1. We did not find any significant difference between the two groups in any sliding window.

The ISC_{NC}/ISC_{SZ} ratios of the 2038 voxels varied with time and exhibited peaks at 89 different time points of the video. To summarize the results, these temporal locations were separated into 18 video segments according to their closeness (temporal locations closer than 3 time points were deemed as one location). Fig. 3C and F present exemplary contents in two of the 18 video segments. Correspondingly, Fig. 3D and G present the voxels that had their peak ISC_{NC}/ISC_{SZ} ratios falling into the presented video segments. Fig. 3E and H show the ISC time courses for the NC and SZ groups at the peak voxels. In all 18 segments, we observed significantly higher ISC in the NC than in the SZ groups. These results indicate that for different voxels, synchronized brain activities in the NC

group could be evoked by different contents in the video.

3.3. Synchronized brain activity templates from normal participants

To avoid averaging across the SZ participants in statistical comparisons, we built spatiotemporal synchronized brain activity templates only from the NC participants and compared individual SZ participants with the NC template. For each of the 2038 voxels, we averaged, across the 44 NC participants, the BOLD signals within the sliding window showing the peak ISC_{NC}/ISC_{SZ} values. Fig. 4A presents an example of the averaged BOLD signals using a blue curve. The averaged BOLD signal from the SZ group is also shown in red to demonstrate the brain activity difference between the groups, which was not used in any statistical inferences. Compared with the SZ group, the averaged signals of the NC group seemed to show clearer fluctuations in the given time windows.

At the corresponding spatiotemporal locations, the BOLD signals from all individuals were correlated to the averaged BOLD signal. Fig. 4B presents a color-coded matrix showing the resultant correlation co-efficients, where the rows represent individuals from both NC and SZ groups, and the columns represent the 2038 voxels. The NC participants consistently exhibited high correlation coefficients, while the SZ participants showed considerable heterogeneity. With this spatiotemporal template from NC, we could characterize each individual using a 2038 dimensional vector, and inter-individual distance could be visualized (see Fig. 4C) by using multi-dimensional scaling (MDS) that compress the high-dimensional space into two dimensions. It should be noted that Fig. 4A–C aim to provide intuitive demonstrations in order to understand the operations in the training dataset. Conclusions cannot be drawn from these demonstrations, because these demonstrations were not independent from the features selection.

3.4. Identifying schizophrenia based on movie-evoked brain activity

The above findings were all generated using the discovery dataset. Using the independent verification dataset (10 SZ and 10 NC), we examined the performance of identifying schizophrenia participants using the spatiotemporal brain activity template of NC participants. An SVM classifier was trained using the 2038-dimensional features in the discovery dataset to classify SZ from NC participants. When applied to the validation dataset, the classifier achieved an accuracy of 95%, a sensitivity of 100%, and a specificity of 90% when identifying SZ participants. The participants in the verification dataset are also presented in the MDS plot using circled dots in Fig. 4C. The colors of the circles indicate the guess of the classifier, and the colors of the dots mark the diagnosis of the participants. Fig. 4D shows the weights of the voxels of interest in the linear classifier, which could be interpreted as "importance" of the voxels in the classifier. The posterior midline structures, the right angular gyrus, the left middle temporal gyrus, and the right dorsal frontal played important roles in the classification.

We examined the generalizability of this approach and the effects of the parameters used in the model, such as the width of the sliding window and the ratio of selected voxels among all voxels using a 5-fold cross-validation scheme. As presented in Fig. 4E, the mean accuracy of the cross-validation ranged from 0.71 to 0.78, depending on the width and ratio. With a width of 30 TRs and a ratio of 0.1, the classifier achieved the highest accuracy of 0.78. A ratio of 0.035 was the closest to the number of selected voxels in the above analyses (2038). At this ratio, the width did not alter the classification accuracy dramatically. Fig. 4E also presents the classification accuracies for the static ISC approach. When less voxels were selected, the static ISC approach gave lower classification accuracies than the sliding-window approach.

3.5. Linking the video contents to abnormal regions in SZ

To interpret the brain regions showing significant ISC difference between the NC and SZ groups, for each of the 11 clusters, we correlated the
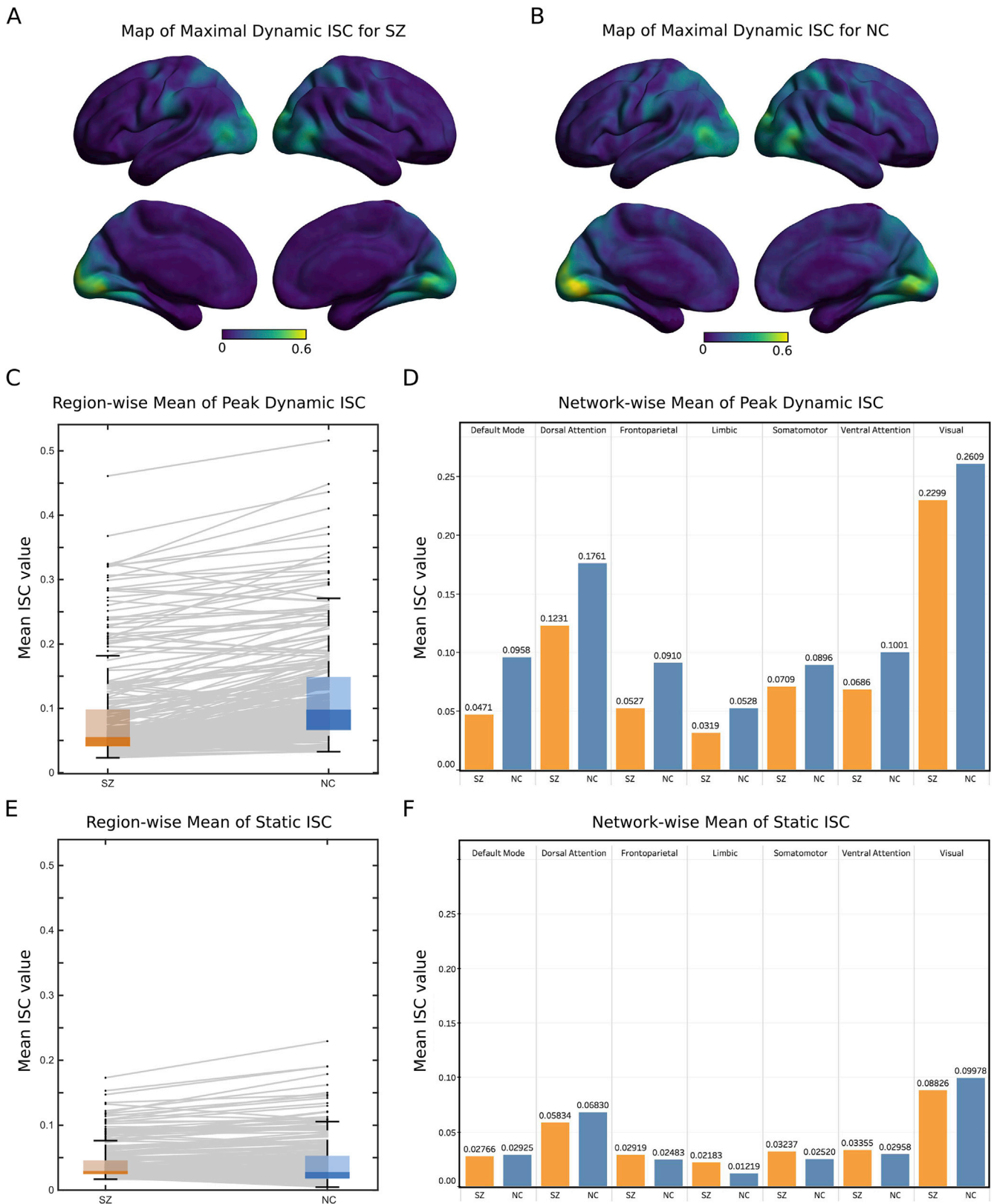
Fig. 2. Inter-subject correlations in the SZ and NC groups. (A) Voxel-wise map of the peak dynamic ISC of the SZ group. (B) Voxel-wise map of the peak dynamic ISC of the NC group. (C) Region-wise comparison of the peak dynamic ISC. (D) Network-wise comparison of the peak dynamic ISC. (E–F) Region-wise and network-wise comparisons of the static ISC that was computed using the whole time series.
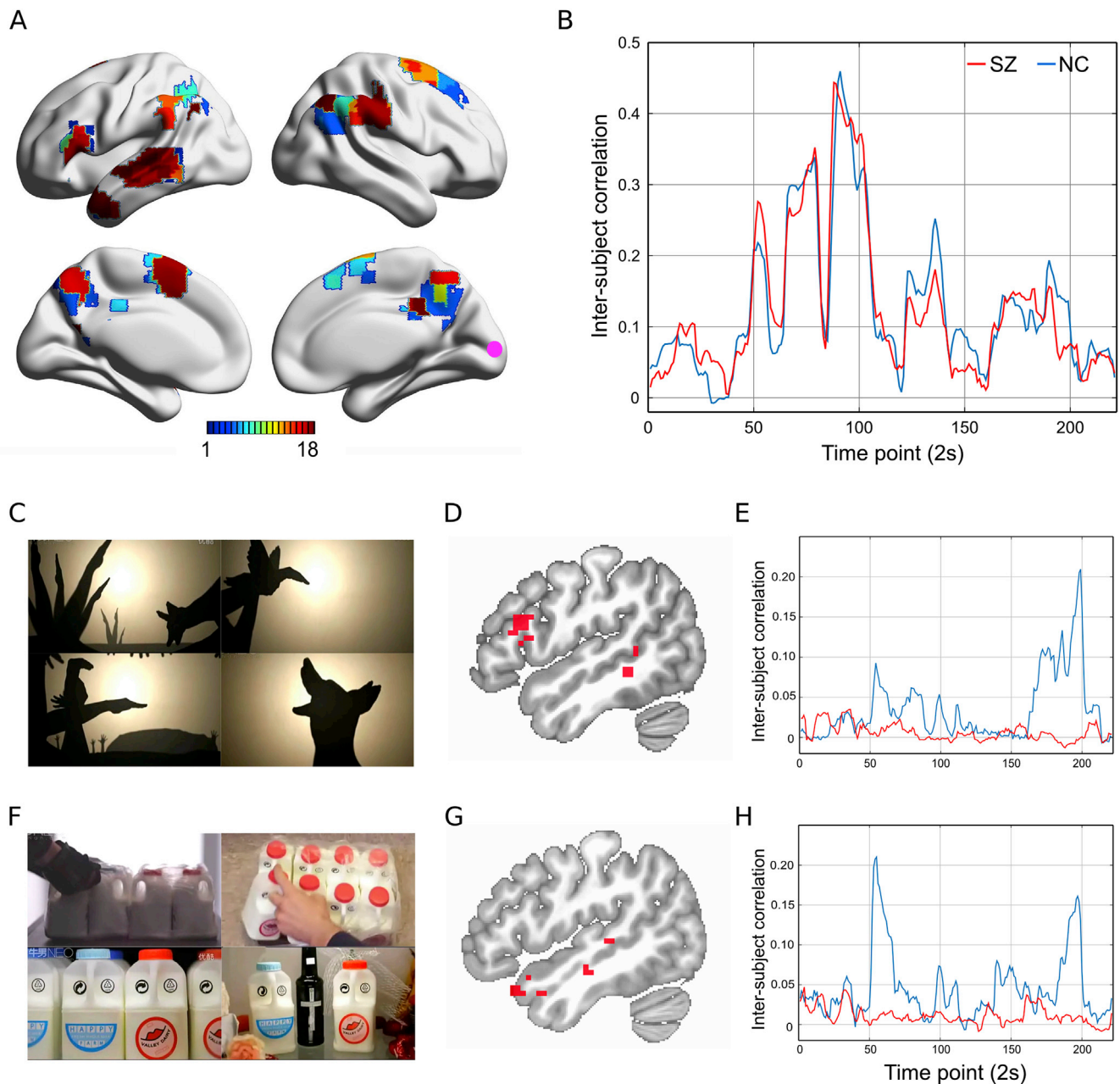
Fig. 3. Spatiotemporal characteristics of the between-group difference of ISC. (A) The surface map shows brain regions where the maximal ISC$_{NC}$/ISC$_{SZ}$ ratios were significant (family-wise error corrected, voxel-wise p < 0.005, one-tailed, cluster size > 88 voxels). The ISC$_{NC}$/ISC$_{SZ}$ peaks of these regions appeared in 89 different time points that were merged into 18 segments. The colors label the segment numbers. B. The inter-subject correlation time courses of the schizophrenia (SZ, red curve) and normal control (NC, blue curve) groups at a voxel in the primary visual area. The two groups showed similar inter-subject correlation time courses, indicating that the natural stimuli were input to the neural system in similar ways between the two groups. C and F present exemplary contents in two of the 18 video segments. D and G show voxels that exhibited maximal ISC$_{NC}$/ISC$_{SZ}$ ratios in the corresponding segments. E and H depict inter-subject correlation time courses of the peak voxels of SZ (red curves) and NC (blue curves) groups.

occurrence of the ISC$_{NC}$/ISC$_{SZ}$ peaks among the 18 segments with a 9-item scale of subjective experience. Twenty college students and graduates (not involved in the study) rated the 18 segments on the following 9 aspects: (1) Feel happy (10-point scale, same below); (2) Feel Angry; (3) Feel fearful; (4) Feel disgusting; (5) Feel sad; (6) Feel emotional fluctuation; (7) Is about myself; (8) Feel empathy; (9) Require reasoning to understand (2 alternatives). Fig. 5 presents a correlation matrix showing the associations between the ISC$_{NC}$/ISC$_{SZ}$ peaks and characteristics of the video content, where correlation coefficients are color-coded and two levels of significance of the correlation coefficients (p < 0.05 and p < 0.01) are marked using different symbols. The left middle temporal gyrus exhibited associations with the reasoning process and the happy

experience, while the right inferior parietal and the right middle frontal gyrus (BA6) showed an association with negative emotional experience such as angry, fearful, disgusting, and sad. The data for obtaining these results are presented in Supplementary Fig. 2. These findings suggest that compared with SZ individuals, NC individuals have more synchronized brain activities in these regions when responding to reasoning and negative emotions.

4. Discussion

In this study, we developed an individualized psychiatric neuro-imaging approach by leveraging inter-subject neural synchronization
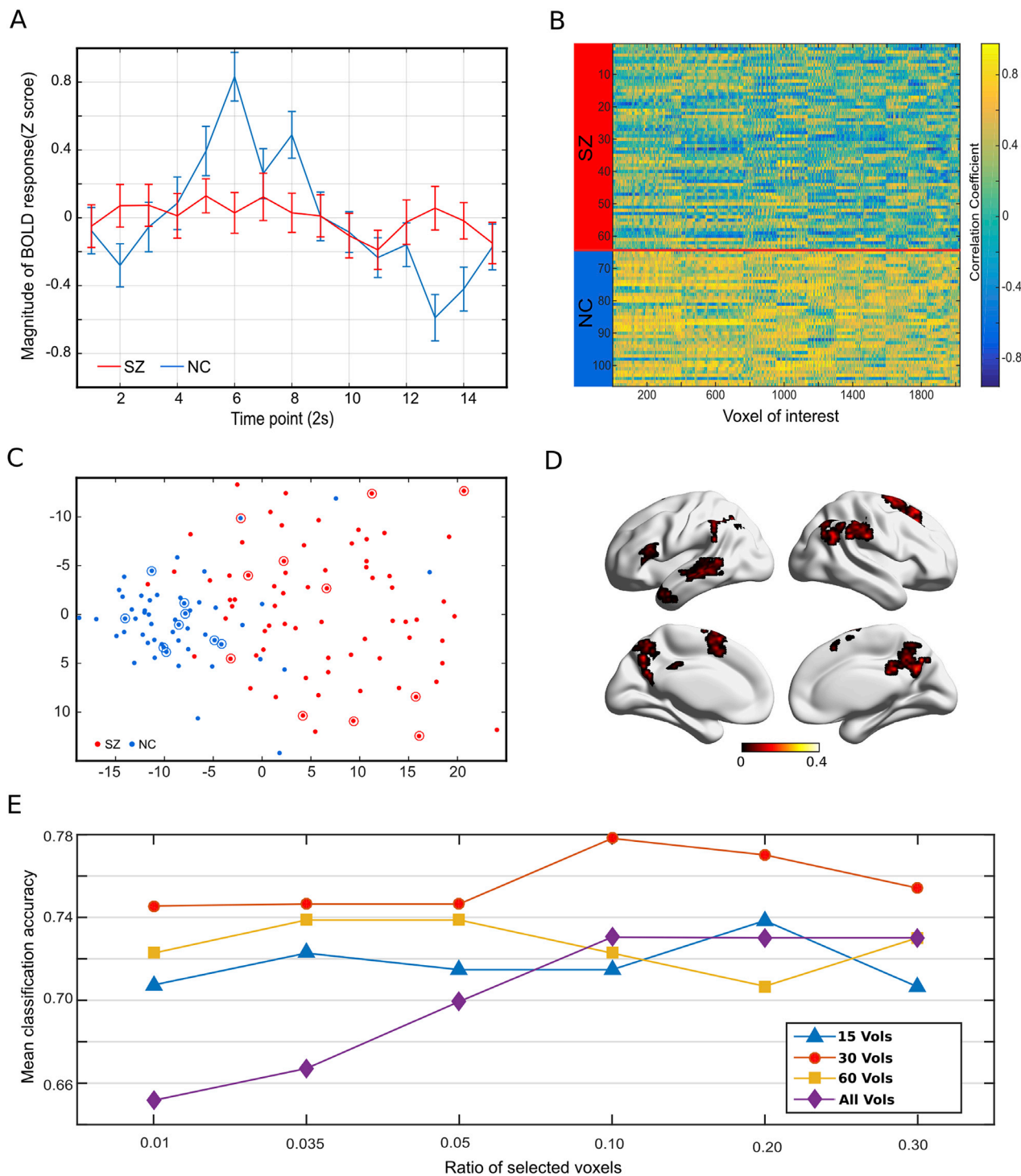
Fig. 4. "NC template" and classification results. (A) An example of "NC template": the mean BOLD time courses from a representative voxel with significant ISC$_{NC}$/ISC$_{SZ}$ peaks. The time courses of the NC individuals were extracted from the time windows showing the peak ISC$_{NC}$/ISC$_{SZ}$ ratios and were standardized into Z scores before averaging. The error bars indicate standard error across individuals. The mean time courses of NC (blue curve) is considered as an "NC template" that represents common brain activities evoked by the natural stimuli in the normal control population. (B) Correlation coefficients between individual brain activity and the NC templates. Each row represents an individual in the discovery dataset (62 SZ and 44 NC), and each column indicates a voxel of interest. (C) Two-dimensional visualization of the inter-subject relationship based on the matrix shown in (B). The NC individuals (blue dots) are closer to each other than the SZ individuals (red dots). The individuals from the independent verification dataset (10 SZ and 10 NC) are also included in this visualization, as marked by the circles. The colors of the circles indicate the guesses of the classifier. The classifiers correctly labeled all but one individual (the blue dot with a red circle). It should be noted that panels (A–C) aim to demonstrate the operations in the training dataset, and conclusions cannot be drawn from these demonstrations (expect the dots with circles in panel C), because these demonstrations were not independent of the features selection. (D) A voxel-wise weight map shows the "importance" of the voxels of interest to the linear classifier. (E) Mean classification accuracy in a 5-fold cross-validation analysis. The horizontal axis represents the ratio of selected voxels. A ratio of 0.035 is the closest to the 2038 voxels selected in the analyses presented in panels (A–D). The performance of different widths of the sliding-window (15, 30, 60, and all volumes) are presented using different lines.
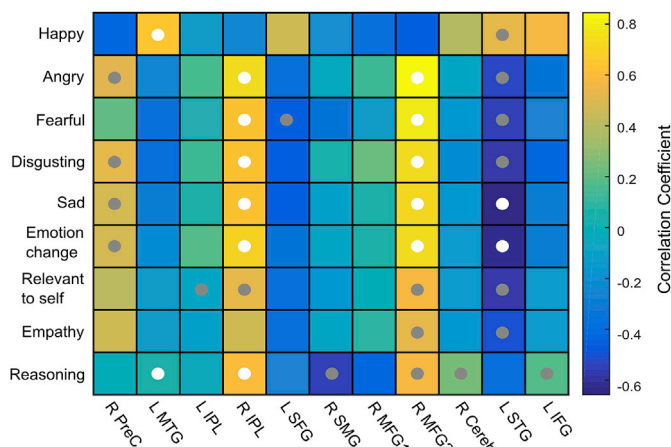
Fig. 5. Associations between the synchronized brain activity in healthy controls and subjective rating scores of the natural stimuli. The brain regions are the 11 clusters identified with significant ISC_{NC}/ISC_{SZ} peak ratios, i.e., higher inter-subject correlation in the NC than in the SZ groups. The colors code the correlation coefficients. The white dots mark the correlation with a significance of $p < 0.01$ and the grey dots with a significance of $p < 0.05$. These associations indicate that NC individuals have more synchronized brain activities than SZ individuals in these regions when responding to reasoning demand and negative emotions when viewing the video. Abbreviations: R PreC: right precuneus; L MTG: left middle temporal gyrus; L IPL: left inferior parietal lobule; R IPL: right inferior parietal lobule; L SFG: left superior frontal gyrus; R SMG: right superior marginal gyrus; R MFG: right middle frontal gyrus; R Cereb: right cerebellum; L STG: left superior temporal gyrus; L IFG: left inferior frontal gyrus.

during the movie watching. A normative template of brain activity for detecting individuals with schizophrenia was constructed by averaging synchronized brain activities among mental healthy individuals while watching movie clips. Abnormal "fingerprints" of psychiatric individuals were then depicted using deviations from the normative template. Our approach yielded a relatively high accuracy in identifying first-episode schizophrenia patients. The advantages of this method, as well as its potential applications, are discussed below.

Group comparison is a classic design in scientific research to reflect the generalizable differences between populations, but the effect size of a populational difference could be affected by the within-group heterogeneity. In neuroimaging studies of psychiatric disorders, the within-group heterogeneity is likely to be high because patients with similar clinical manifestations may not share common neural characteristics (Cusi et al., 2012). Due to the considerable heterogeneity, the low effect size in group comparisons requires the increased demand on large sample size and high reliability of the measure (Kanyongo et al., 2007), and some demands are not realistic in current psychiatric neuroimaging studies. Thus, conventional approaches based on group mean comparison limit its applications in psychiatric neuroimaging.

The methodology in the present study avoids averaging data of psychiatric patients, thus has the potential to protect the large heterogeneity in neural characteristics among individuals of certain psychiatric disorders. Such heterogeneity is actually informative under some circumstances, which can be used to detect brain functional abnormality in individual patients. There are several methods that have been successfully implemented in the field of functional neuroimaging to characterize individual differences. For instance, Wang et al. (2018) have used individual-specific functional connectivity measures to characterize the individual difference in psychotic patients, and Russel et al. and Braga et al. have demonstrated the gain of precision in investigating accumulated brain scans of single individuals (Braga and Buckner, 2017; Poldrack, 2017). In comparison to the existing individualized methods, our strategy based on inter-subject neural synchronization treats healthy and psychiatric individuals differently in that our approach attempts to evoke synchronized brain activities in the mentally healthy population, the

possibility of which has been demonstrated in previous studies (e.g., Hasson, 2004; Nguyen et al., 2019; Byrge et al., 2015; Vanderwal et al., 2017). For the individual psychiatric individuals, our approach does not aim to examine their "averaged" deficits but to reveal their individual differences from the common brain activities in the healthy population.

Outcomes from our approach are significant as it possesses several strengths as compared with previously available methods. First, comparing with the commonly used resting-state measures that are derived from uncontrolled mental states, this paradigm minimized the individual difference of the mentally healthy population and thus increased the effect size of the comparison. The application to identify individuals with schizophrenia provided supporting evidence for the effectiveness of this methodology. Consistent with this notion, we observed that naturalistic stimuli evoked more synchronized brain activity in the NC participants than in the SZ patients and that comparing the brain activities of individual SZ patients with the common brain activity of NC participants yielded a high accuracy in identifying SZ patients. Second, comparing individual participants with a common template could be applied to other structural (see an excellent example in Wolfers et al., 2018) and functional metrics, though the naturalistic paradigm is a good companion for this strategy. Third, comparing with the widely used resting-state paradigm, brain activities evoked by naturalistic stimuli can be directly compared or averaged across subjects, and the data acquisition is as easy as the resting-state. Finally, comparing with the repetitive task-activation paradigm, the naturalistic paradigm induces much richer cognitive and social contents and can potentially evoke more detailed individual differences in psychiatric patients (Byrge et al., 2015; Mäntylä et al., 2018).

It is worthy to note that the methodology presented here has limited power in explanation of the individual differences in brain activity. Although the coding of natural stimuli provides an approach to associate synchronized brain activity to various variables, it is not sufficient to provide an affirmative answer to why an individual patient's brain activity deviates from the healthy population. Nonetheless, the capability which reveals individual differences and the potential to accurately identify psychiatric patients makes this methodology a useful tool for translational neuroimaging studies on psychiatric disorders with considerable heterogeneity. Although previous evidence has suggested that content-rich tasks may perform better in identifying individuals based on brain activity (Finn et al., 2017), in future works, we still need some direct comparisons between the naturalistic and the resting-state paradigms when applying normative model to identify individuals with mental disorders. In addition, 57% of the training set were schizophrenia patients, which is much higher than the prevalence of this disease. This disagreement with the real-world situation should be noted when applying the paradigm to develop potential diagnosis tools.

In conclusion, our study demonstrates the advantages of an individualized psychiatric neuroimaging methodology based on inter-subject neural synchronization evoked by viewing natural video clips. This approach respects the heterogeneity in brain activities, which allows us to make inferences for individual patients and has the potential to have more broad applications into translational psychiatric imaging.

Declaration of competing interest

All authors reported no biomedical financial interests or potential conflicts of interest.

Acknowledgement

Appendix A. Supplementary data

Supplementary data to this article can be found online at https://doi.org/10.1016/j.neuroimage.2019.116227.

References

Braga, R.M., Buckner, R.L., 2017. Parallel interdigitated distributed networks within the individual estimated by intrinsic functional connectivity. Neuron 95, 457–471 e5.

Byrge, L., Dubois, J., Tyszka, J.M., Adolphs, R., Kennedy, D.P., 2015. Idiosyncratic brain activation patterns are associated with poor social comprehension in autism. J. Neurosci. 35, 5837–5850.

Carlson, J.M., Rubin, D., Mujica-Parodi, L.R., 2017. Lost emotion: disrupted brain-based tracking of dynamic affective episodes in anxiety and depression. Psychiatry Res. Neuroimaging 260, 37–48. https://doi.org/10.1016/j.pscychresns.2016.12.00217.

Cusi, A.M., Nazarov, A., Holshausen, K., Macqueen, G.M., McKinnon, M.C., 2012. Systematic review of the neural basis of social cognition in patients with mood disorders. J. Psychiatry Neurosci. 37, 154–169.

Finn, E.S., Scheinost, D., Finn, D.M., Shen, X., Papademetris, X., Constable, R.T., 2017. Can brain state be manipulated to emphasize individual differences in functional connectivity? Neuroimage 160, 140–151.

Gordon, E.M., Laumann, T.O., Gilmore, A.W., Newbold, D.J., Greene, D.J., Berg, J.J., et al., 2017. Precision functional mapping of individual human brains. Neuron 95, 791–807 e7.

Hasson, U., 2004. Intersubject synchronization of cortical activity during natural vision. Science 303, 1634–1640 (80-).

Insel, T., Cuthbert, B., Garvey, M., Heinssen, R., Pine, D.S., Quinn, K., et al., 2010. Research domain criteria (RDoC): toward a new classification framework for research on mental disorders. Am. J. Psychiatry 167, 748–751.

Isik, L., Singer, J., Madsen, J.R., Kanwisher, N., Kreiman, G., 2018. What is changing when: decoding visual information in movies from human intracranial recordings. Neuroimage 180 (August 2017), 147–159. https://doi.org/10.1016/j.neuroimage.2017.08.027.

Kanyongo, G.Y., Brook, G.P., Kyei-Blankson, L., Gocmen, G., 2007. Reliability and statistical power: how measurement fallibility affects power and required sample sizes for several parametric and nonparametric statistics. J. Mod. Appl. Stat. Methods 6, 81–90.

Kapur, S., Phillips, A.G., Insel, T.R., 2012. Why has it taken so long for biological psychiatry to develop clinical tests and what to do about it? Mol. Psychiatry 17, 1174–1179.

Lahnakoski, J.M., Glerean, E., Jääskeläinen, I.P., Hyönä, J., Hari, R., Sams, M., Nummenmaa, L., 2014. Synchronous brain activity across individuals underlies shared psychological perspectives. Neuroimage 100, 316–324.

Mäntylä, T., Nummenmaa, L., Rikandi, E., Lindgren, M., Kieseppä, T., Hari, R., et al., 2018. Aberrant cortical integration in first-episode psychosis during natural audiovisual processing. Biol. Psychiatry. https://doi.org/10.1016/j.biopsych.2018.04.014.

Mueller, S., Wang, D., Fox, M.D.D., Yeo, B.T.T.T.T., Sepulcre, J., Sabuncu, M.R.R., et al., 2013. Individual variability in functional connectivity architecture of the human brain. Neuron 77, 586–595.

Nguyen, M., Vanderwal, T., Hasson, U., 2019. Shared understanding of narratives is correlated with shared neural responses. Neuroimage 184, 161–170.

Poldrack, R.A., 2017. Precision neuroscience: dense sampling of individual brains. Neuron 95, 727–729.

Power, J.D., Fair, D.A., Schlaggar, B.L., Petersen, S.E., 2010. The development of human functional brain networks. Neuron. https://doi.org/10.1016/j.neuron.2010.08.017.

Spaulding, W., Deogun, J., 2011. A pathway to personalization of integrated treatment: informatics and decision science in psychiatric rehabilitation. Schizophr. Bull. 37, S129–S137.

Thomas Yeo, B.T., Krienen, F.M., Sepulcre, J., Sabuncu, M.R., Lashkari, D., Hollinshead, M., et al., 2011. The organization of the human cerebral cortex estimated by intrinsic functional connectivity. J. Neurophysiol. 106 (3), 1125–1165. https://doi.org/10.1152/jn.00338.2011.

Vanderwal, T., Eilbott, J., Finn, E.S., Craddock, R.C., Turnbull, A., Castellanos, F.X., 2017. Individual differences in functional connectivity during naturalistic viewing conditions. Neuroimage 157, 521–530.

Wang, D., Li, M., Wang, M., Schoeppe, F., Ren, J., Chen, H., et al., 2018. Individual-specific functional connectivity markers track dimensional and categorical features of psychotic illness. Mol. Psychiatry 1.

Wolfers, T., Doan, N.T., Kaufmann, T., Alnæs, D., Moberget, T., Agartz, I., et al., 2018. Mapping the heterogeneous phenotype of schizophrenia and bipolar disorder using normative models. JAMA Psychiatry 75, 1146.